

Dynamic evolution of flow structures and viscosity during basaltic magma emplacement and crystallization in an upper-crustal sill



Dynamic evolution of flow structures and viscosity during basaltic magma emplacement and crystallization in an upper-crustal sill

LeeAnn Srogi¹, Arianna Soldati², Tim Lutz³, Nikolas Watson¹, and Meagen Pollock³

¹Dept. Earth-Space Sciences, West Chester Univ.; ²Dept. Marine-Earth-Atmospheric Sciences, North Carolina State Univ.; ³Dept. Geology, College of Wooster



1. Introduction

Click HERE for a brief audio summary of the entire poster.

0:00 / 2:44

Summary: Magma reservoirs are thought to be readily crystallized for much of their lifetime.

OPEN

2. Crystal mush and flow macro- and micro-structures

Summary: In the decimeter-scale quarry near the base of the 36-Peters sill (BPS), hundreds of millimeter-scale plagioclase- and perovskite-rich nodules (PRL, PQL) occur along toes of dikes. In water-saturated flow tubes, plagioclase nodules resemble very fine-grained crystallizations of plagioclase intergrowth (Carter and Marsh, 2011). Microstructural evidence that internal flow was the primary process, and more important than crystallization, shows peritectic crystallization of plagioclase (PLAG) in PRL, and that in nodules, plagioclase (PLAG) grew in a relatively large range of PLAG growth temperatures.

OPEN

3. Crystallization stages: mineral compositions and textures

Summary: Key changes in mineral compositions are linked to stages of magmatic system evolution in real, in-situ, and experimental studies. Basaltic magmas crystallize relatively slowly; layered crystal mush in the 36-Peters sill developed after basaltic magmas. Change in crystal compositions from PRL to nodules is linked to an around 100°C temperature interval in PRL formation.

Figure 3.1: Plagioclase composition and zoning patterns are consistent throughout all dike-branch nodules and perovskite stages of melt crystallization. Figures in Sections 3.4 and 3.5 show that in Sections 3.1, 3.2, and 3.3, the perovskite nodules formed on stages related to PLAG zoning.



Figure 3.1: Plagioclase compositions, phenocryst cores are consistent throughout all

OPEN

4. P-T estimates, alpha-MELTS modeling, and crystallinity

Summary: Results of thermodynamic calculations (Pati et al., 2008; Hesse and Pichler, 2017) are consistent with crystallization at low or mid levels, as suggested for related rhyolites (e.g., Hesse et al., 2010). CPX (phenocrysts formed in-magma) and melt at ca. 120 MPa. All remaining minerals crystallized in upper crust at 200-30 MPa. Applications of MELTS modeling (Sisson and Hesse, 1995; Hesse and Chatterjee, 2008; Gualini et al., 2012) finds average Jackwerth (nodules) with 0.5 wt% H₂O (the dike branch PLAG) and AUG (nodules) and Tergovist (but not CPX), and evidence for an interval of crystal and liquid loss from the BPS, probably resulting from magmatic transport.

Fig. 4.1: Pressure-Temperature estimates for CPX, PLAG, AUG, and CPX.



Figure 4.1: Pressure-Temperature estimates for CPX, PLAG, AUG, and CPX.

OPEN

5. Viscosity modeling and evolving mush rheology

Summary: Viscosity models were calculated for Liquid (Dietrich et al., 2008) and crystal suspension (Mason and Duggan, 2014) for stages of melt crystallization. These show that viscosity was likely during formation of nodules with aligned PLAG and melt, but would have increased viscosity, but this cannot be modeled with these equations. Vol. % crystals, maximum viscosity values for nodules during the PLAG melt crystallization stage, viscosity cannot be calculated for crystallization and later stages.

Hesse, insight into mush rheology after PRL.

OPEN

6. Conclusions

Summary: The present a range of system development for crystallization in a sill. Internal structure is mobile and upper crust (Figure 6.1). Three major findings are summarized in Figure 6.1.



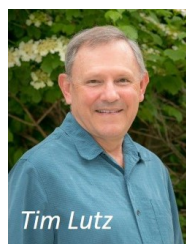
Figure 6.1: Summary of findings

OPEN

CHART INFO REFERENCES CONTACT AUTHOR PRINT GET POSTER

LeeAnn Srogi¹, Arianna Soldati², Tim Lutz¹, Nikolas Watson¹, and Meagen Pollock³

¹Dept. Earth-Space Sciences, West Chester Univ.; ²Dept. Marine-Earth-Atmospheric Sciences, North Carolina State Univ.; ³Dept. Geology, College of Wooster



PRESENTED AT:



1. INTRODUCTION

Click [HERE](#) for a brief audio summary of the entire poster.

Summary: Magma reservoirs are thought to be mostly crystalline for most of their lifetimes. Sub-volcanic intrusions are logical places to study crystal mushes, but plutonic rocks are overprinted and incomplete records that need to be interpreted within the context of an entire magmatic system. We find an appropriate upper-crustal magma system comprising a sill-dike network from basalt down to a sill intruded at 5.5-6 km (Section 1). The network is part of the 201.5 Ma Central Atlantic Magmatic Province (CAMP), a global-scale magmatic event associated with rifting of Pangaea.

This poster focuses on solidified basaltic crystal mush (*diabase* = *dolerite* = *gabbro*) in an upper-crustal sill and associated sub-volcanic plumbing system. A general history of the magmatic system, and evolution of mush composition and rheology during crystallization, are developed using field evidence (Sections 2 and 5), mineral compositions and petrography (Section 3), P-T estimates and thermodynamic modeling (Section 4), and crystallinity estimates and viscosity modeling (Sections 4-5).

Figure 1-1: Maps and information about the Central Atlantic Magmatic Province in Eastern North America and the study area in the Newark basin.

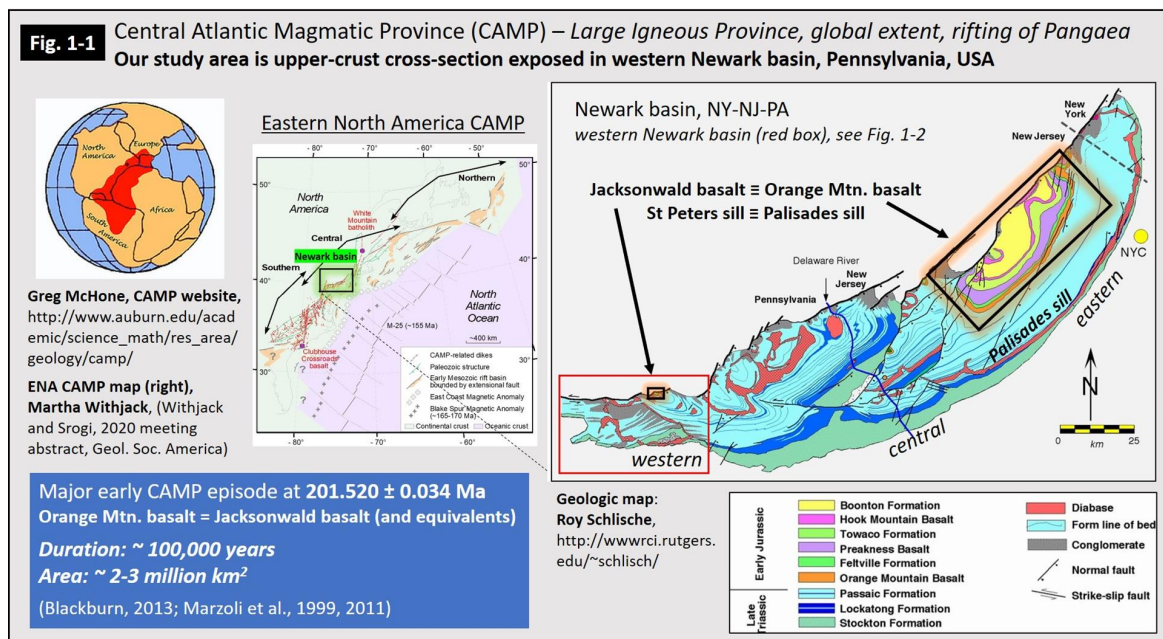
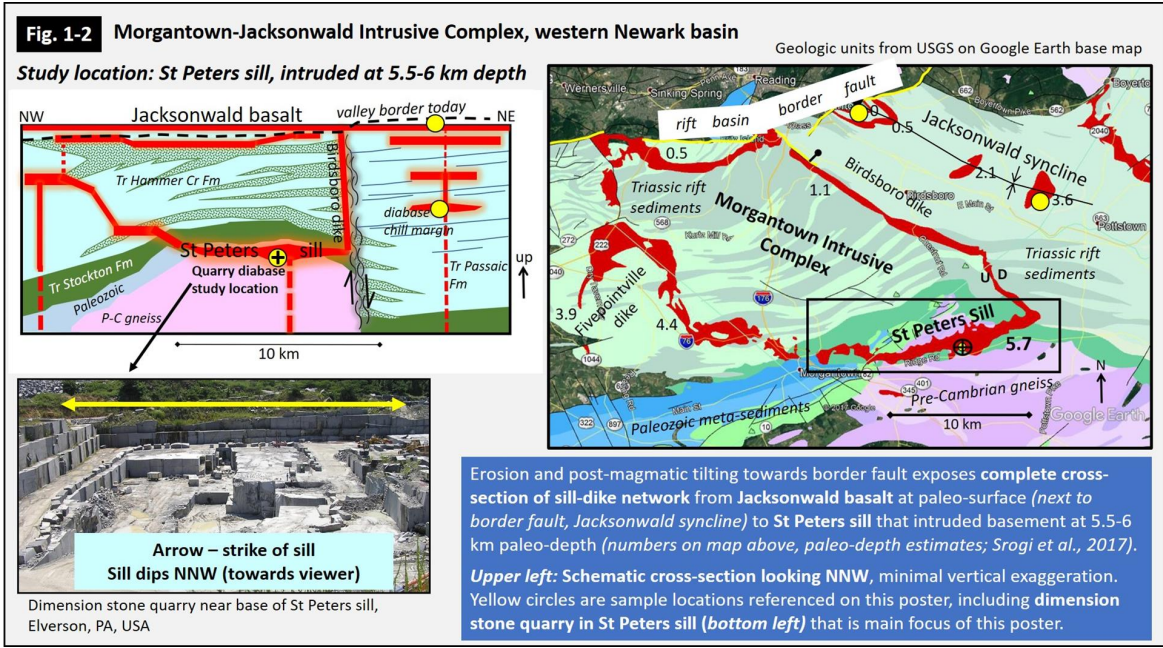


Figure 1-2: Maps and cross-sections showing the entire upper-crust sill-dike network exposed in the western Newark basin, and the St Peter's sill comprising the crystal mush that is the focus of this poster.



2. CRYSTAL MUSH AND FLOW: MACRO- AND MICRO-STRUCTURES

Summary: In the dimension stone quarry near the base of the St Peters sill (SPS), hundreds of millimeter-scale plagioclase- and pyroxene-rich modal layers (PRL, PXL) occur along tops of decimeter- to meter-scale flow lobes. Macro-structures resemble wax-in-gelatin simulations of pulsed magmatic intrusion (Currier and Marsh, 2015). Microstructural evidence that lateral flow was the primary process and more important than compaction includes: shape-preferred orientations of plagioclase (PLAG) in PRL parallel to inclined layer margins; tiling of PLAG grains; wrapping and pressure shadows of PLAG around larger pyroxene (PX) grains within PRL. Microstructures resemble spindle viscometer experiments using bimodal analog particle slurries (Cimarelli et al., 2011).

Figure 2-1: Location and information about dimension stone quarry near base of SPS. The quarry measures roughly 60m x 50m, with a total of about 20m vertical exposure.

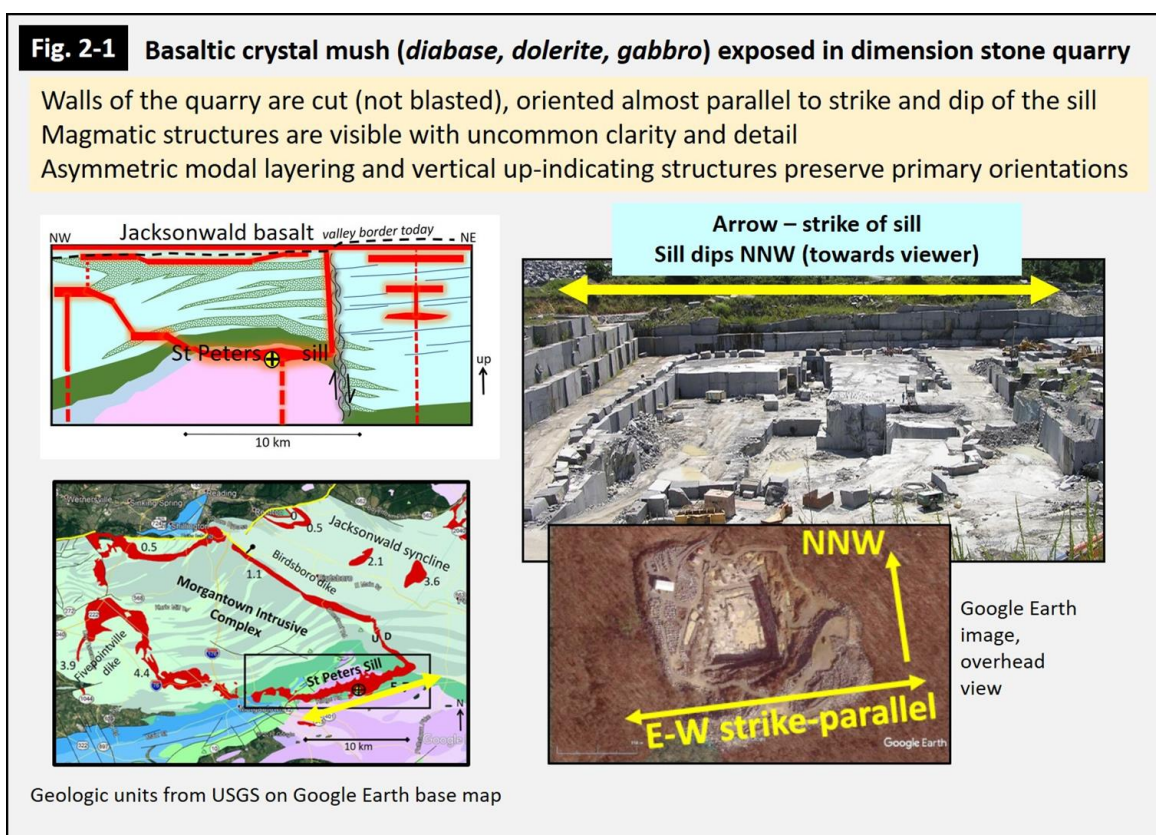


Figure 2-2: Macro-structures - plagioclase-rich layers (PRL) and flow lobes - in diabase crystal mush in the SPS dimension stone quarry, viewed on wall cut parallel to strike of sill, normal to dip of PRL.

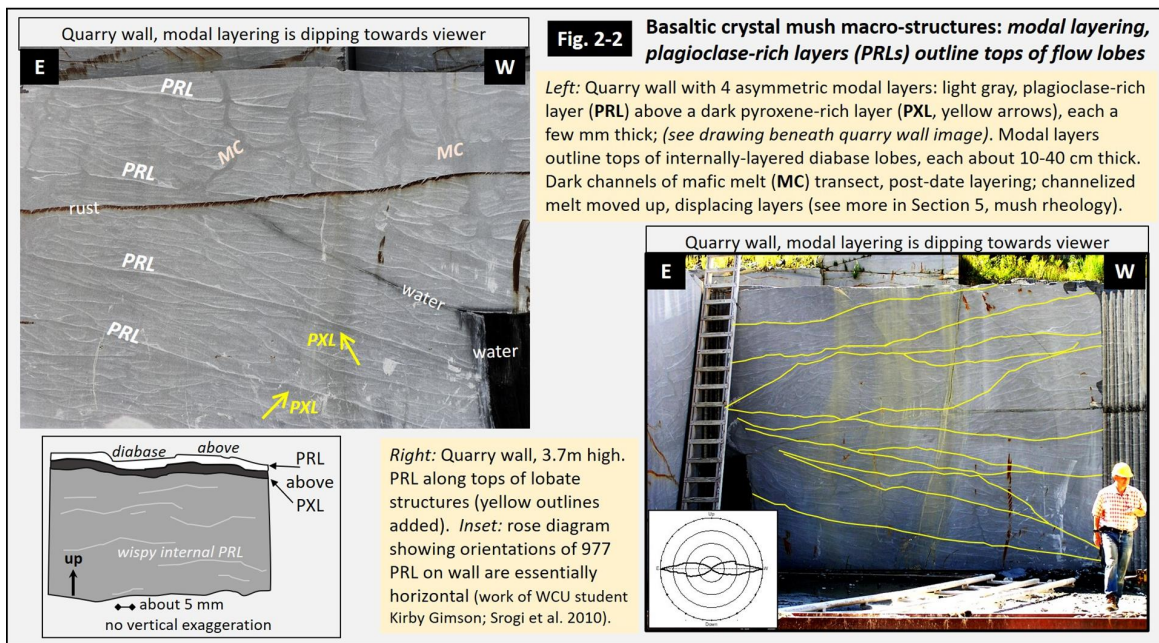


Figure 2-3: Flow lobes viewed on wall cut normal to sill strike and parallel to PRL dip; and on block surface cut at shallow angle (about 20°) to PRL dip. Latter section shows overlapping lobes similar to wax-in-gelatin models of pulsed magmatic flow (Currier and Marsh, 2015). This link may take you to the wax model videos; note especially Videos 3 and 5: Link to videos of wax models, Currier and Marsh (2015) (<http://dx.doi.org/10.1016/j.jvolgeores.2015.07.009>)

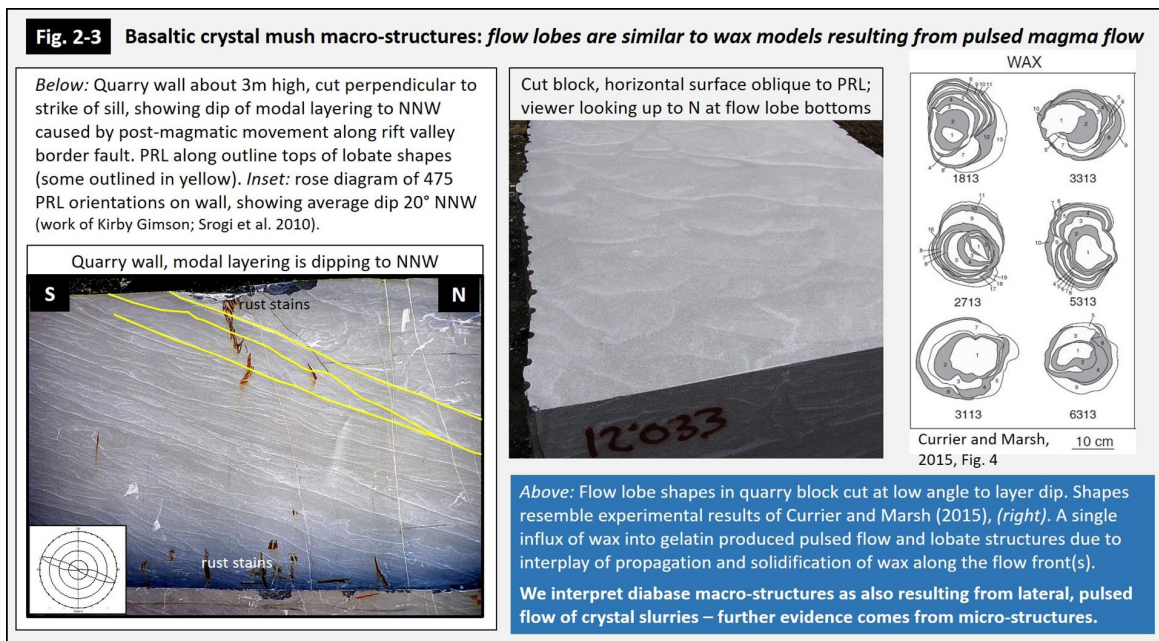
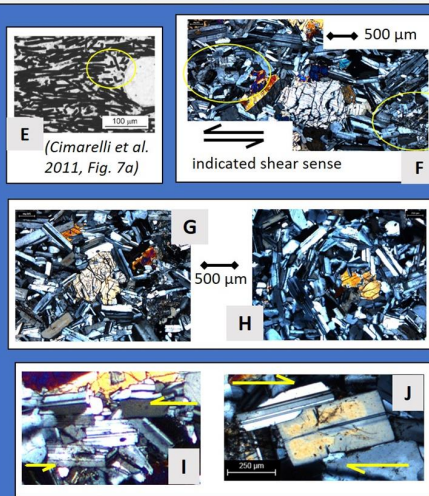
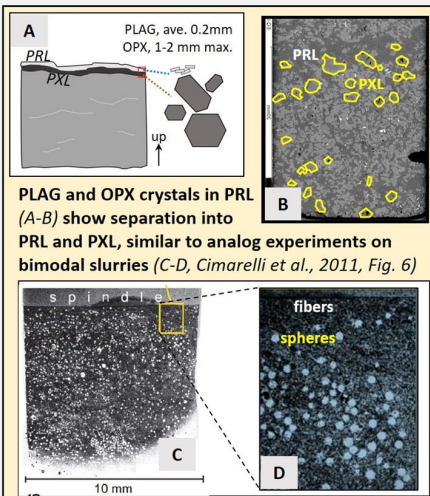


Figure 2-4: Orientation of thin section for viewing and measuring micro-structures in the PRL.

Fig. 2-6 Micro-structures in 3 perpendicular thin sections indicate shear flow within PRL

Flow structures are similar to analog viscometer experiments on bimodal crystal slurries by Cimarelli et al. (2011): shear flow and shear thinning caused separation of small fibers (=PLAG) from larger spheres (=OPX), and flow alignment of fibers



Flow indicators in PRL are similar to analog experiments (E):

Pressure shadows (F, yellow circles) around larger OPX

PLAG wrapping pyroxene in vertical (G) and plan view (H)

Tiling of PLAG grains, one of the best flow indicators, in vertical (I) and plan views (J)

Shear sense indicators are consistent with lateral flow and spreading, mainly from east to west and south to north

3. CRYSTALLIZATION STAGES: MINERAL COMPOSITIONS AND TEXTURES

Summary: Key changes in mineral composition are linked to stages of magmatic system evolution in mid-to-deep and upper crust. Basalt eruption occurred relatively early; layered crystal mush in the St Peters sill developed after basalt eruption. Change in augite compositions from Fe-enrichment trend to an unusual Ca-enrichment trend is linked to PRL formation.

Figure 3-1: Plagioclase composition and zoning patterns are consistent throughout sill-dike-basalt network and preserve stages of mush crystallization. Figures in Sections 3-4, and data tables in Sections 3-5, use consistent color scheme based on stages related to PLAG zoning.

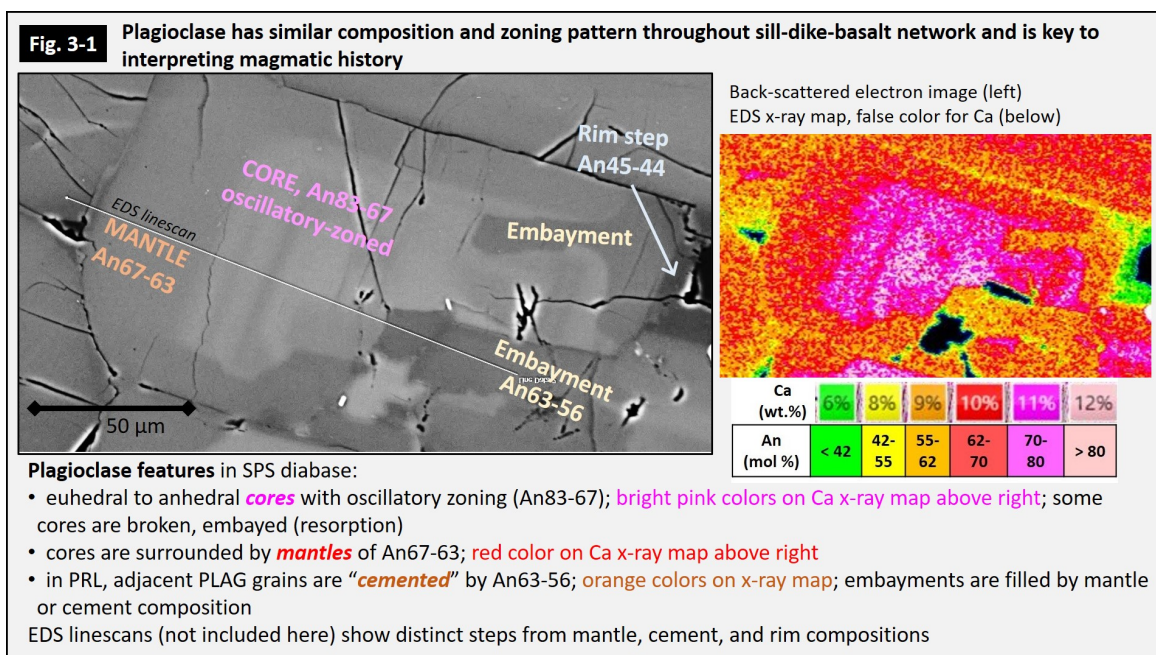


Figure 3-2: Pyroxene compositions: phenocryst cores are consistent throughout sill-dike-basalt network; 2 trends are identified for augite (AUG).

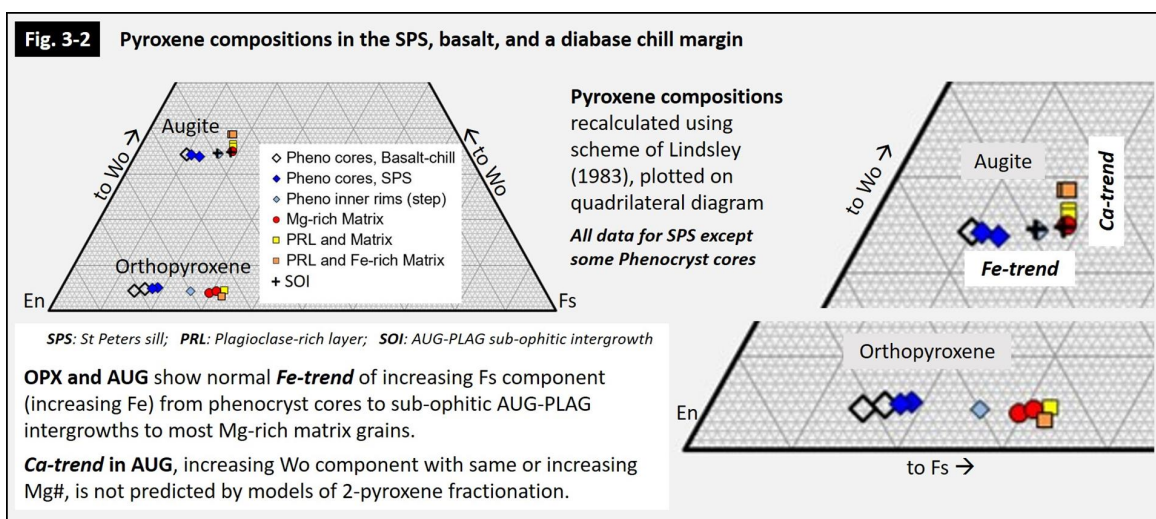


Figure 3-3: Similar early-formed crystal cargo in Jacksonwald basalt and St Peters sill demonstrates volcanic-plutonic link and relative timing of eruption(s) in history of this magma system.

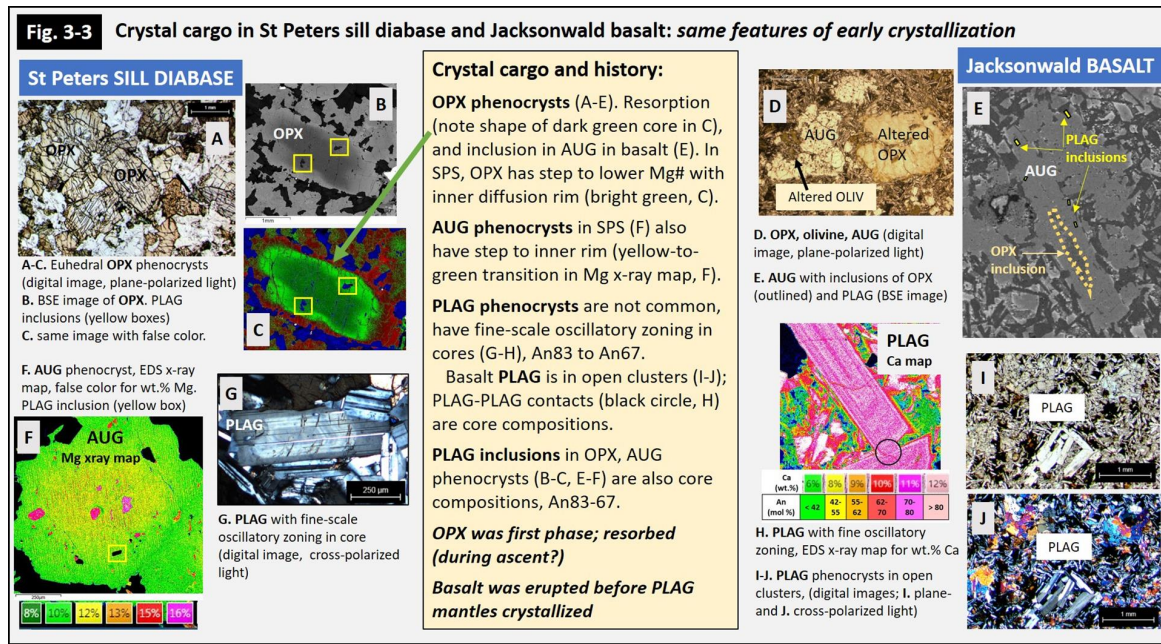


Figure 3-4: During and after eruption(s) came an active interval of multiple resorption and recharge events. Crystallization resumed with growth of plagioclase mantles and augite following the Fe-enrichment trend.

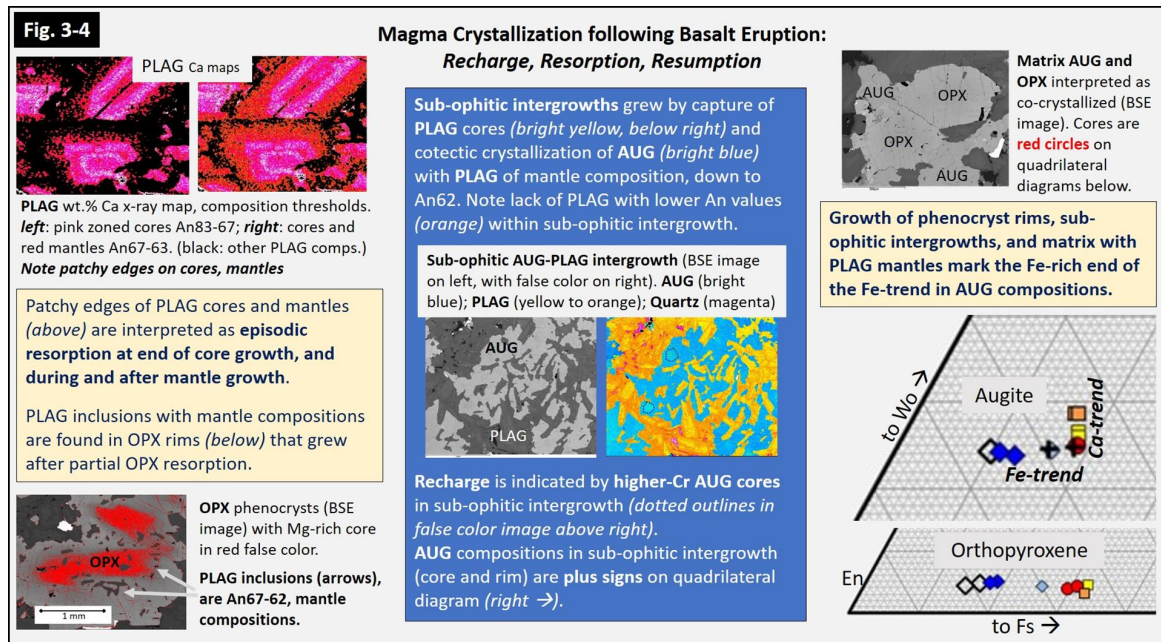
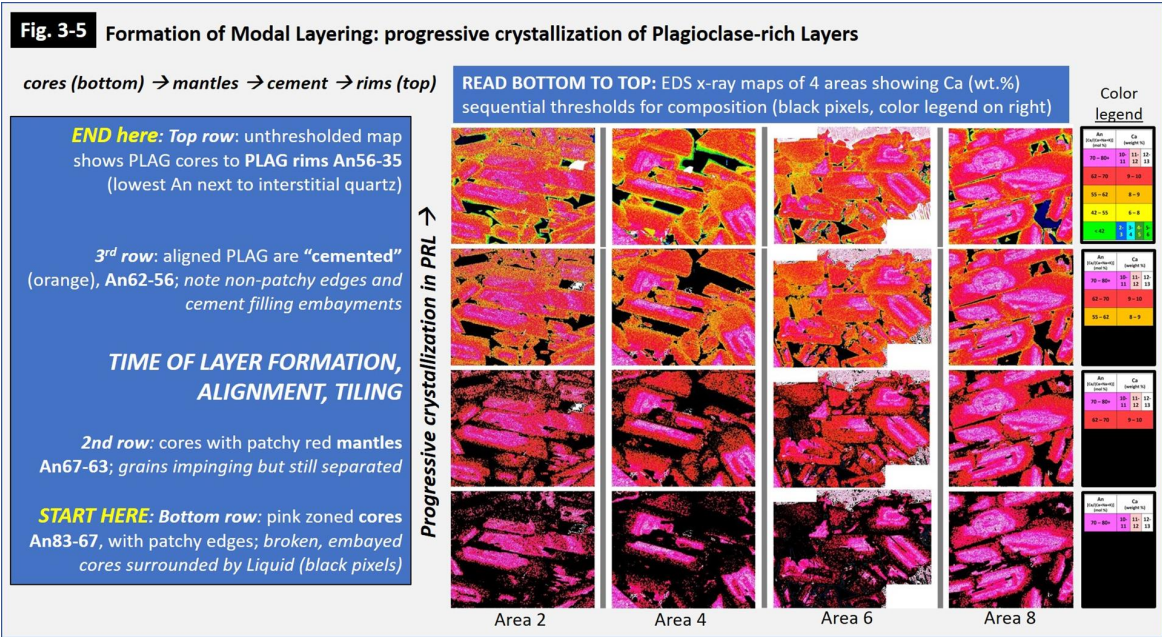


Figure 3-5: Ca x-ray maps with composition thresholds show the progressive growth of plagioclase in 4 areas of a plagioclase-rich layer (PRL). Timing of PLAG alignment and PRL formation is identified: after PLAG mantles and before cementation of the PRL.



4. P-T ESTIMATES, ALPHA-MELTS MODELING, AND CRYSTALLINITY

Summary: Results of thermobarometry calculations (Putirka, 2008; Neave and Putirka, 2017) are consistent with crystallization at two crustal levels, as suggested for related rift magmatism (e.g., Heinonen et al., 2019). OPX phenocrysts formed in middle-deep crust at ca. 500 MPa. All remaining minerals crystallized in upper crust at 200-10 MPa. Application of MELTS modeling (Ghiorso and Sack, 1995; Asimow and Ghiorso, 1998; Gualda et al., 2012) finds average Jacksonwald basalt with 0.5 wt.% H₂O fits diabase PLAG and AUG compositions and Temperatures (but not OPX), and evidence for an interval of crystal and liquid loss from the SPS, probably resulting from magma transport.

Fig. 4-1: Pressure-Temperature calculation results for OPX-Liquid, AUG-Liquid, and OPX-AUG.

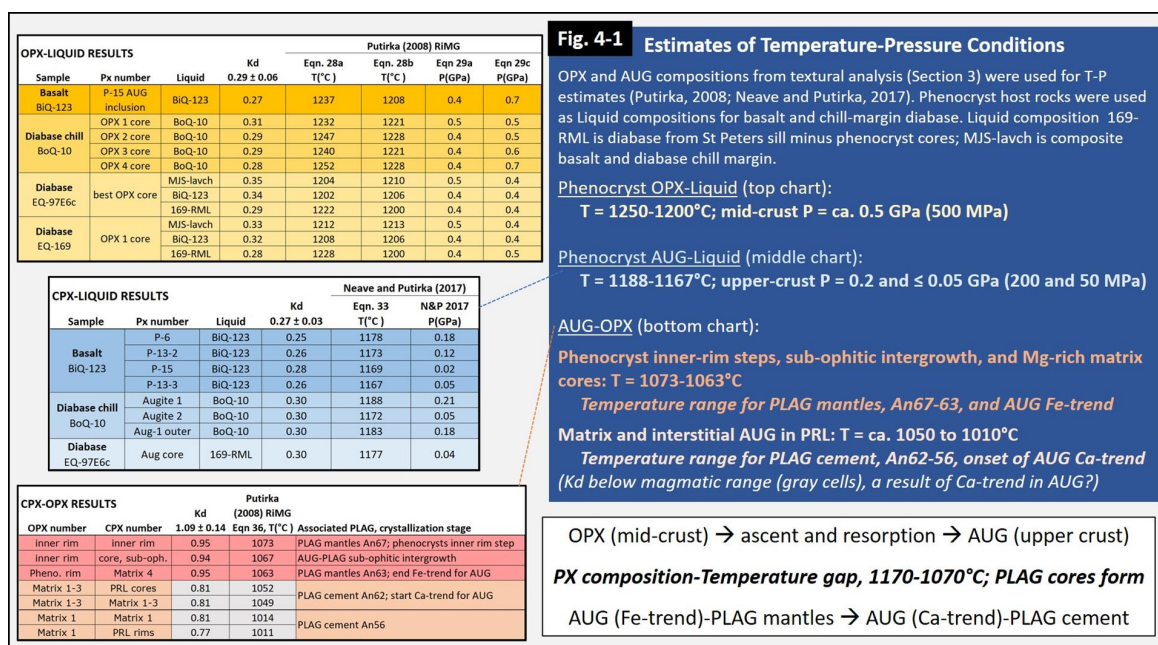


Figure 4-2: A total of 35 alpha-MELTS models (Ghiorso and Sack, 1995; Asimow and Ghiorso, 1998; Gualda et al., 2012) were run: average Jacksonwald basalt Liquid AB3 with 0.5 wt.% H₂O fits the diabase PLAG and AUG compositions and Temperatures (but not OPX).

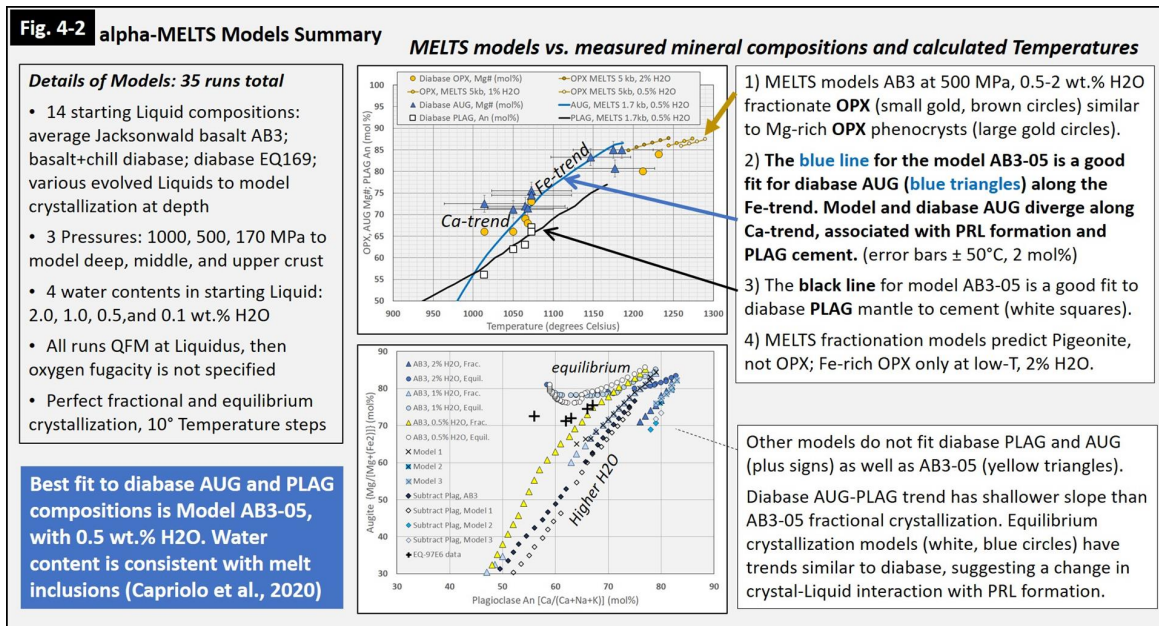


Figure 4-3: MELTS model AB3 predicts 30-35 vol.% pyroxenes crystallized in the interval between pyroxene cores and matrix (Temp. = 1170-1070°C). However, diabase contains only 5-8 vol.% pyroxenes with these compositions. Magma transport and eruption during this interval would explain "missing" pyroxenes and be consistent with textural evidence from PLAG cores which were forming at that time.

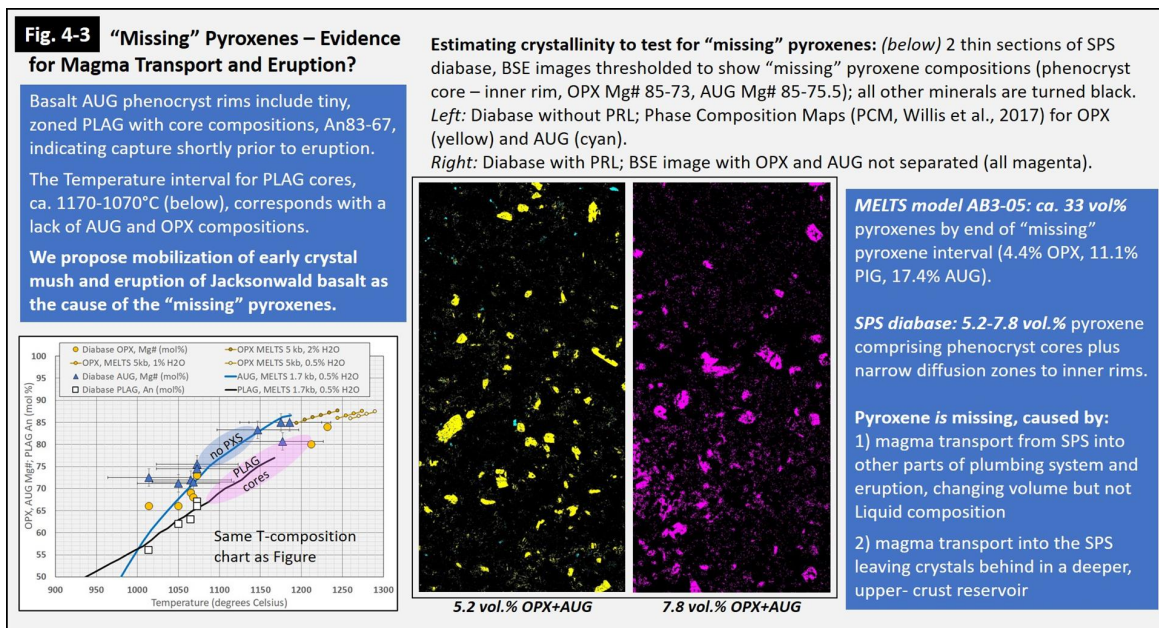


Figure 4-4: Estimates of volume % crystals in diabase and PRL from sample images and MELTS models.

Fig. 4-4 Crystallinity must be estimated before using a viscosity model for crystal suspensions

Stages of crystallization identified from composition-texture analysis, P-T estimates, MELTS models.

Jacksonwald basalt AB3 used as initial Liquid composition and as starting Liquid in all MELTS models shown here.

Vol.% crystals estimated from MELTS uses model output: Liquid composition, fractionated mineral mass and density.

Vol.% crystals estimated from diabase samples and PRL based on thresholding BSE images in ImageJ for mineral compositions corresponding with stages in crystallization history.

- Best estimates come from the diabase Phase Composition Maps, which are BSE images calibrated by EDS analyses and processed to generate separate images for PLAG, OPX, and AUG (Willis et al., 2017). Diabase PCM does not include a PLAG-rich layer (PRL).
- Vol.% crystals in diabase with PRL and the entire PLAG-rich layer (across the thin section) estimated by thresholding BSE image of all minerals using PCM images and thresholds as a guide.
- Vol.% crystals in the 4 areas of the PRL (see Figure 3-5) estimated by thresholding Ca x-ray maps for PLAG composition.

Crystallinity (volume % crystals) for MELTS models, Diabase samples, PRLs

Stage in crystallization history	MELTS AB3 1.0 wt.% H ₂ O			MELTS AB3 0.5 wt.% H ₂ O			Diabase PCM no PRL			Diabase BSE with PRL			PRL entire PLAG+PXS			PRL 4 areas PLAG only		
	PXS	PLAG	Total	PXS	PLAG	Total	PXS	PLAG	Total	PXS	PLAG	Total	PXS	PLAG	Total	PXS	PLAG	Total
Liquidus, 500 MPa	0	0	0.0	0	0	0.0							no PRL at these stages			no PRL at these stages		
after OPX crystals, 500 MPa	4.0	0	4.0	4.3	0	4.3	4.9	0	4.9	4.9	0	4.9						
ascent, resorption, 170 MPa	4.0	0	4.0	4.0	0	4.0	2.5	0	2.5	2.5	0	2.5						
erupted basalt, AUG Mg83.5	22.6	4.0	26.6	22.2	8.8	31.0												
after PLAG cores, An83-67	MELTS model not good fit			32.9	18.61	51.5	5.2	18.4	23.6	7.8	19.6	27.3						
after PLAG mantles, An67-63				37.0	26.7	63.7	12.7	29.6	42.4	20.4	31.3	51.8	11.6	46.8	58.4	0.0	63.9	63.9
after PLAG cement, An63-56				39.2	31.1	70.3	36.9	39.7	76.6	39.0	44.3	83.3	20.2	67.6	87.8	0.0	86.9	86.9

5. VISCOSITY MODELING AND EVOLVING MUSH RHEOLOGY

Summary: Viscosity models were calculated for Liquid (Giordano et al., 2008) and crystal suspensions (Moitra and Gonnermann, 2014) for stages of mush crystallization. Shear thinning behavior was likely during formation of modal layers with aligned PLAG and would have reduced viscosity, but this cannot be modeled with these equations. Vol.% crystals exceeds maximum values for random packing after PLAG mantle crystallization stage; viscosity cannot be calculated for cementation and later stages.

However, insight into mush rheology after PRL formation and cementation comes from macro-structures in the diabase quarry. Increased viscosity and rigidity of crystal mush changed intrusive style of younger magma inputs from lateral sheet flow to channelized vertical flow.

Figure 5-1: Calculated viscosity and consistency results for Liquid and crystal suspensions, respectively.

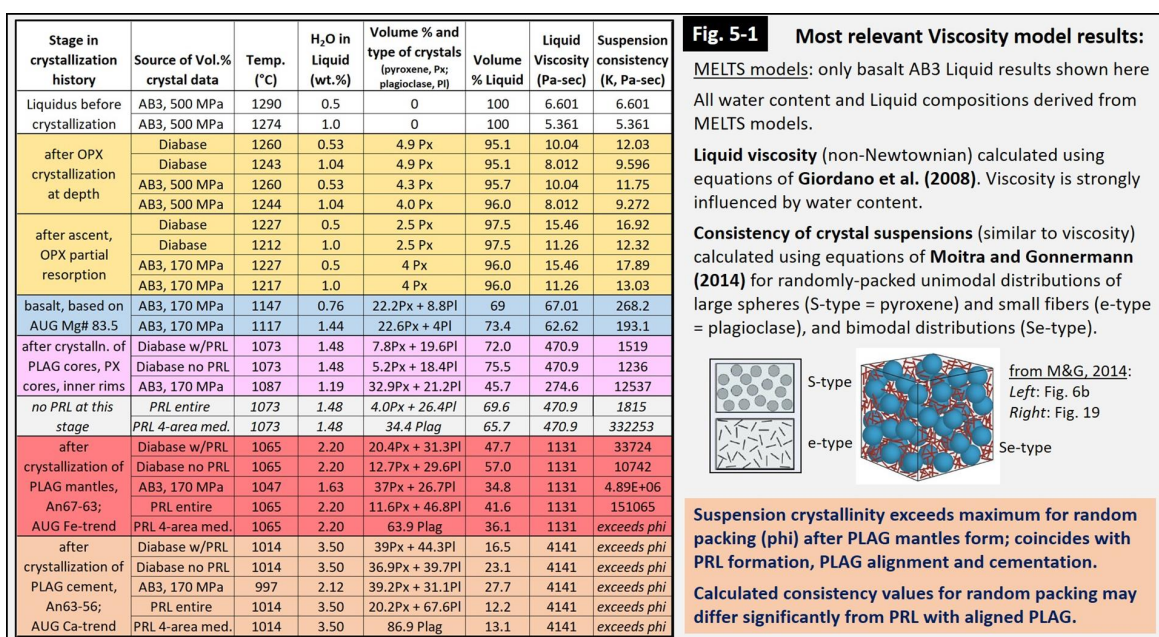


Figure 5-2: Chart showing how calculated viscosity (or consistency) increases as Temperature decreases in basaltic Liquid (no crystals) and magma with crystals up to PLAG mantle crystallization stage.

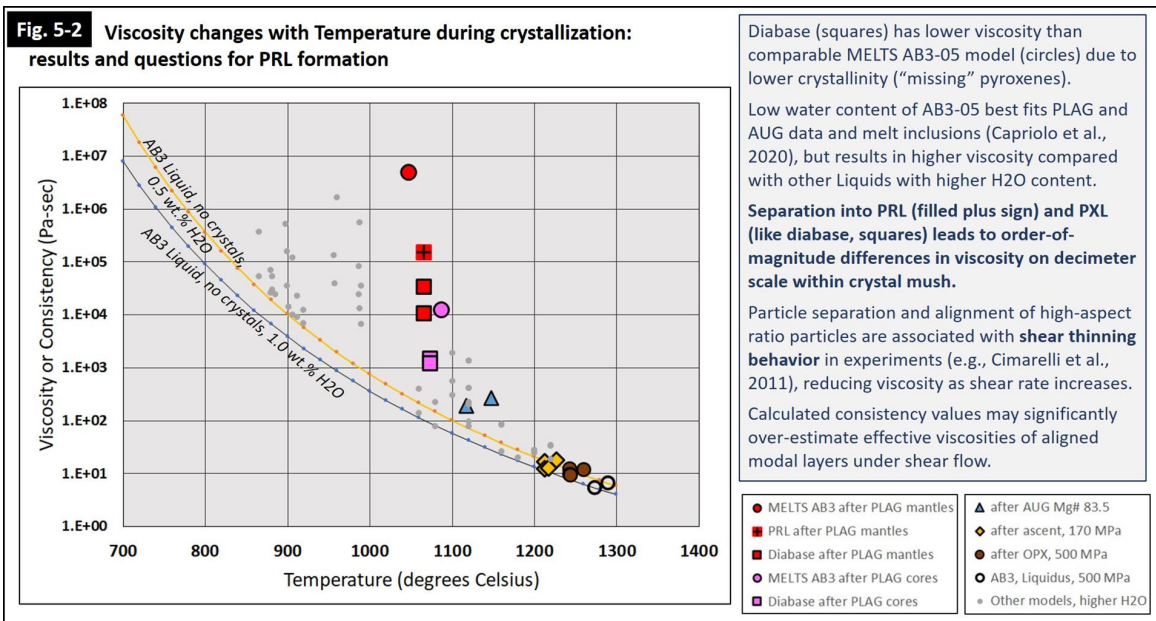


Figure 5-3: Macro-structures in the diabase quarry provide evidence for the general rheology of the mush after PRL formation. Initial stages: lateral sheet flow of later basaltic inputs into non-rigid but coherent layered mush.

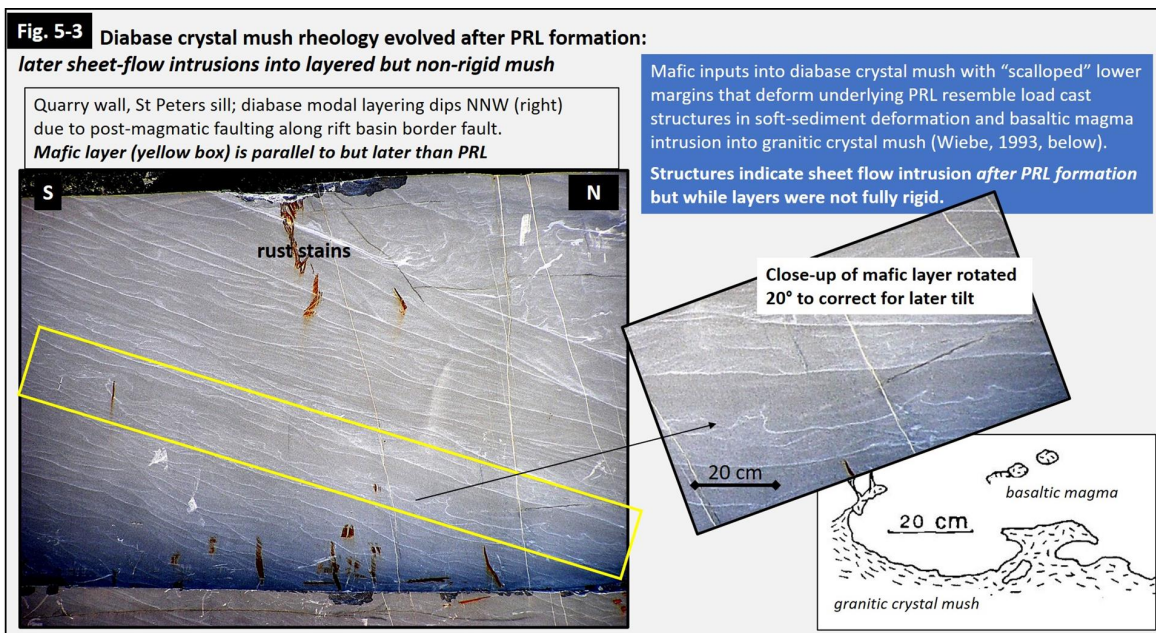


Figure 5-4: Later basaltic sheet cross-cuts more rigid layers and produces drag folds of the PRL in underlying crystal mush.

Fig. 5-4

Diabase crystal mush rheology evolved after PRL formation: later sheet-flow intrusions into mush becoming more rigid

Mafic layer with upper PRL cross-cuts modal layering (best seen on top left).

Underlying modal layers are deformed into drag folds (yellow lines), indicating some component of east-to-west flow. North-south flow, into-out of plane of image, cannot be evaluated.

East-to-west flow and north-south flow components are also observed in tiling of plagioclase grains in the PRL.

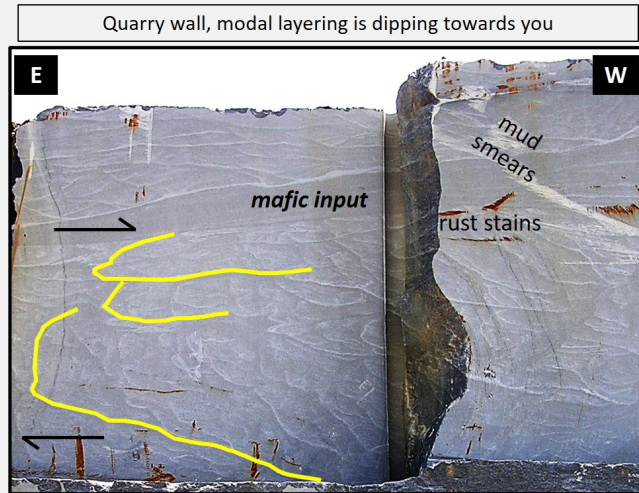
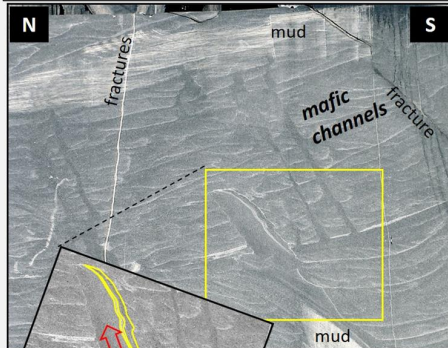


Figure 5-5: Channelized, vertical flow of late-stage basaltic inputs into diabase crystal mush with heterogeneous viscosity and rigidity. Is channelization a sign of decreasing magma flux? Did the mush rheology change the flow regime and prevent later basaltic inputs from rejuvenating the mush and leading to eruption?

Fig. 5-5 Diabase crystal mush rheology evolved after PRL:
later flow was channelized into pipe-like structures

Quarry wall, diabase modal layering dips NNW (left)
Channels of mafic magma cross-cut modal layering



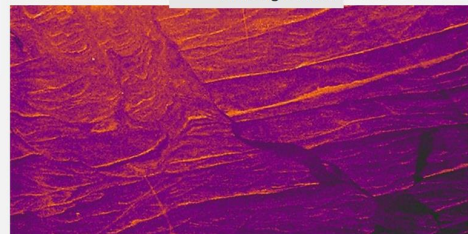
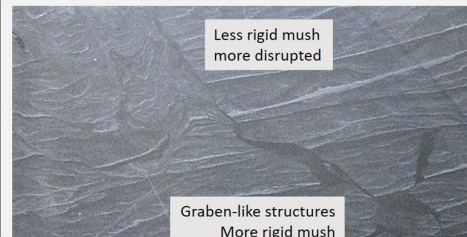
In cross-section, viewed from above, mafic channels are pipe-like, not dike-like PRL dragged up along channel margins outline the channel



Close-up of mafic channel rotated 20° to correct for tilt.
Upward flow (red arrow) deformed mush into drag folds and dragged PRL up along sides of channel (yellow lines).

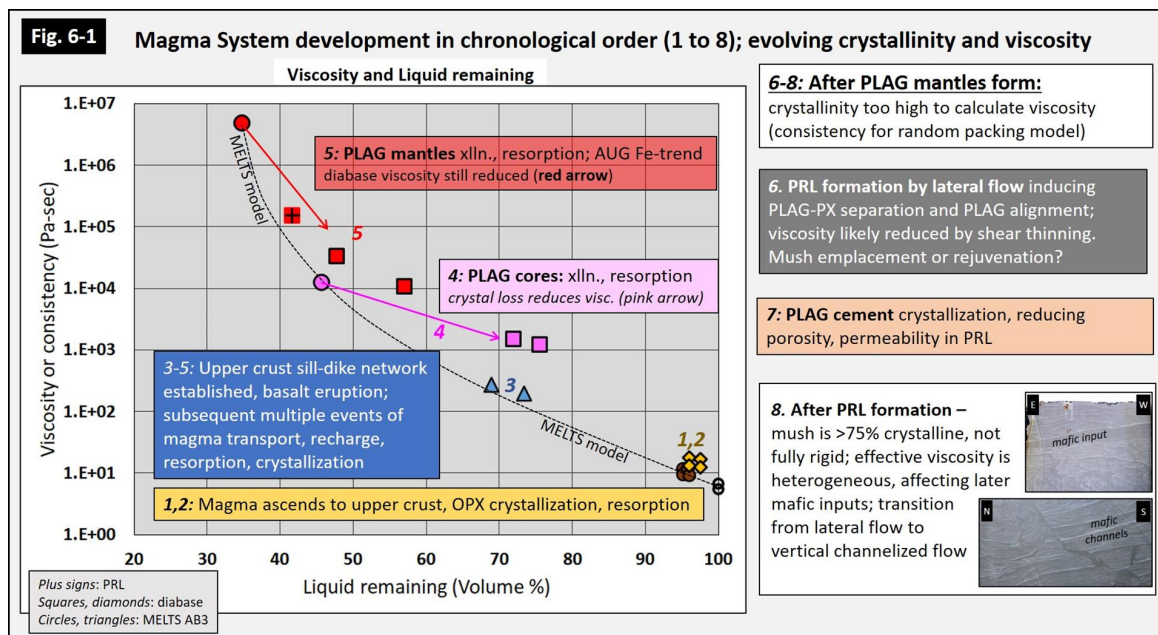
Mafic channels are later structures, as mush became more rigid, perhaps with waning flux of magma into the St Peters sill.

Mush rheology was variable at cm-dm scale (below): transition from graben-like to slump-like structures (highlighted by false color imaging, bottom).



6. CONCLUSIONS

Summary: We propose a magma system chronology for crystallization in a sill-dike-basalt network in middle and upper crust (Figure 6-1). Three major findings are summarized below Figure 6-1.



1) Recharge displaced mush and led to eruption of basalt with crystal cargo relatively early in system history, when crystallinity was 25-35% and viscosity 200-250 Pa-sec. Eruption did not require rejuvenation or mobilization of highly-crystalline mush.

2) Lateral magma flow during later emplacement or rejuvenation of mush in the St Peters sill led to self-organization of flow lobes with modal layering which likely reduced effective viscosity by shear thinning.

3) As the heterogeneous rheology of layered, high-viscosity mush evolved, the behavior of younger magma inputs into the St Peters sill changed from lateral flow to vertical channelized flow; this may have prevented mush rejuvenation and eruption in the last stages of the system history.

REFERENCES

- Asimow, P. D., & Ghiorso, M. A. (1998). Algorithmic modifications extending MELTS to calculate subsolidus phase relations. *American Mineralogist*, 83, 1127-1131.
- Blackburn, T. J., Olsen, P. E., Bowring, S. A., McLean, N. M., Kent, D. V., Puffer, J., McHone, G., Rasbury, E. T., & Et-Touhami, M. (2013). Zircon U-Pb geochronology links the end-Triassic extinction with the Central Atlantic Magmatic Province. *Science*, 340, 941-945.
- Capriolo, M., Marzoli, A., Aradi, L. E., Callegaro, S., Dal Corso, J., Newton, R. J., Mills, B. J. W., Wignall, P. B., Bartoli, O., Baker, D. R., Youbi, N., Remusat, L., Spiess, R., & Szabo, C. (2020). Deep CO₂ in the end-Triassic Central Atlantic Magmatic Province. *Nature Communications*, 11. <https://doi.org/https://doi.org/10.1038/s41467-020-15325-6>
- Cimarelli, C., Costa, A., Mueller, S., & Mader, H. M. (2011). Rheology of magmas with bimodal crystal size and shape distributions: Insights from analog experiments. *Geochemistry, Geophysics, Geosystems*, 12(7). <https://doi.org/10.1029/2011GC003606>
- Currier, R. M., & Marsh, B. D. (2015). Mapping real time growth of experimental laccoliths: The effect of solidification on the mechanics of magmatic intrusion. *Journal of Volcanology and Geothermal Research*, 302, 211-224.
- Ghiorso, M. A., & Sack, R. O. (1995). Chemical Mass-Transfer in Magmatic Processes .4. A Revised and Internally Consistent Thermodynamic Model for the Interpolation and Extrapolation of Liquid-Solid Equilibria in Magmatic Systems at Elevated Temperatures and Pressures. *Contributions to Mineralogy and Petrology*, 119, 197-212.
- Giordano, D., Russell, J. K., & Dingwell, D. B. (2008). Viscosity of magmatic liquids: A model. *Earth and Planetary Science Letters*, 271, 123-134.
- Gualda, G. A. R., Ghiorso, M. S., Lemons, R. V., & Carley, T. L. (2012). Rhyolite-MELTS: A modified calibration of MELTS optimized for silica-rich, fluid-bearing magmatic systems. *Journal of Petrology*, 53, 875-890.
- Lindsley, D. H. (1980). Pyroxene thermometry. *American Mineralogist*, 68, 477-493.
- Marzoli, A., Jourdan, F., Puffer, J. H., Cuppone, T., Tanner, L. H., Weems, R. E., Bertrand, H., Cirilli, S., Bellieni, G., & De Min, A. (2011). Timing and duration of the Central Atlantic magmatic province in the Newark and Culpeper basins, eastern U.S.A. *Lithos*, 122, 175-188.
- Marzoli, A., Renne, P. R., Piccirillo, E. M., Ernesto, M., Bellieni, G., & De Min, A. (1999). Extensive 200-million-year-old continental flood basalts of the Central Atlantic Magmatic Province. *Science*, 284, 616-618.
- Moitra, P., & Gonnermann, H. M. (2015). Effects of crystal shape- and size-modality on magma rheology. *Geochemistry, Geophysics, Geosystems*, 16, 1-26. <https://doi.org/doi:10.1002/2014GC005554>
- Neave, D. A., & Putirka, K. D. (2017). A new clinopyroxene-liquid barometer, and implications for magma storage pressures under Icelandic rift zones. *American Mineralogist*, 102, 777-794.
- Putirka, K. (2008). Thermometers and barometers for volcanic systems. In K. Putirka & F. Tepley (Eds.), *Minerals, Inclusions, and Volcanic Processes* (pp. 61-120). Mineralogical Society of America. <https://doi.org/DOI:10.2138/rmg.2008.69.3>
- Srogi, L., Lutz, T., Dickson, L. D., Pollock, M., Gimson, K., & Lynde, N. (2010). Magmatic layering and intrusive plumbing in the Jurassic Morgantown Sheet, Central Atlantic Magmatic Province. In G. M. Fleegeer & S. J. Whitmeyer (Eds.), *The Mid-Atlantic Shore to the Appalachian Highlands: Field Trip Guidebook* (pp. 51-68). Geological Society of America.
- Srogi, L., Martinson, P. J., Willis, K. V., Lutz, T., Kulp, R., & Pollock, M. (2017). The 201-Ma magma plumbing system in the western Newark basin: how and (maybe) why it's different from the east. 34th annual meeting of the Geological Association of New Jersey, West Chester, Pennsylvania.
- Watson, N., Srogi, L., Lutz, T., & Gimson, K. (2019). Textural study reveals dynamic development of mineral layering and crystal alignments by magmatic flow in a diabase sheet, western Newark Basin, Pennsylvania, USA [conference abstract]. annual national meeting, Geological Society of America, Phoenix, Arizona, USA.

Wiebe, R. A. (1993). Basaltic injections into floored silicic magma chambers. EOS, Transactions of the American Geophysical Union, 74(1), 1,3.

Willis, K. V., Srogi, L., Lutz, T., Monson, F. C., & Pollock, M. (2017). Phase composition maps integrate mineral compositions with rock textures from the micro-meter to the thin section scale. Computers and Geosciences, 109C, 162-177.